Article

Outgassing and eruption of basaltic magmas: The effect of conduit geometry

PIOLI, Laura, *et al*.

Abstract

The flow dynamics of magmas is controlled by several parameters, including magma rheology, density, surface tension, gas and liquid flow rate, and the geometry of the flow field, which is mainly regulated by the conduit shape. For this reason, magmatic flows along fissures and dikes are significantly different from those along axisymmetric conduits. Basaltic eruptions are typically fed by fractures or dike systems that reach the surface, giving rise to fissure eruptions. Scaled experiments show that in these low-viscosity systems, gas transport and segregation (i.e., the outgassing dynamics) are deeply controlled by the fracture geometry. Rapid bubble clustering and formation of bubble plumes determine the formation of lateral magma convection cells involving up to 70 vol% of the melt. In analogy with outgassing in cylindrical conduits, the average vesicularity and size of bubbles increase with increasing gas flow rate and melt viscosity and density, which also control the lateral extent of the bubble plume and convection cells.

Reference

PIOLI, Laura, *et al*. Outgassing and eruption of basaltic magmas: The effect of conduit geometry. *Geology*, 2017, p. G38787.1

DOI : 10.1130/G38787.1

THE GEOLOGICAL SOCIETY OF AMERICA®

Outgassing and eruption of basaltic magmas: The effect of conduit geometry

L. Pioli[1]*, B.J. Azzopardi[2]†, C. Bonadonna[1], M. Brunet[3], and A.K. Kurokawa[4]
[1]Departement des Sciences de la Terre, Université de Genève, 1205 Geneva, Switzerland
[2]Faculty of Engineering, University of Nottingham, Nottingham NG7 2RD, UK
[3]Laboratorie de Géologie des Systèmes Volcaniques, Institut de Physique du Globe de Paris, 75005 Paris, France
[4]National Research Institute for Earth Science and Disaster Resilience, Tsukuba, Ibaraki, 305-0006, Japan

ABSTRACT

The flow dynamics of magmas is controlled by several parameters, including magma rheology, density, surface tension, gas and liquid flow rate, and the geometry of the flow field, which is mainly regulated by the conduit shape. For this reason, magmatic flows along fissures and dikes are significantly different from those along axisymmetric conduits. Basaltic eruptions are typically fed by fractures or dike systems that reach the surface, giving rise to fissure eruptions. Scaled experiments show that in these low-viscosity systems, gas transport and segregation (i.e., the outgassing dynamics) are deeply controlled by the fracture geometry. Rapid bubble clustering and formation of bubble plumes determine the formation of lateral magma convection cells involving up to 70 vol% of the melt. In analogy with outgassing in cylindrical conduits, the average vesicularity and size of bubbles increase with increasing gas flow rate and melt viscosity and density, which also control the lateral extent of the bubble plume and convection cells.

INTRODUCTION

Several mafic eruptions are fed by fissures which range in length from a few hundred meters to a few kilometers (Genareau et al., 2010; Reynolds et al., 2016). However, long-lived fissure eruptions (i.e., weeks to months) are very rare because the flow tends to focus into a single or multiple, regularly spaced eruption points which are either stable or migrating with time accompanying fissure extension, such as in the documented cases of the A.D. 1943 Paricutin (Mexico), 1970 Hekla (Iceland), and 2002 Etna (Italy) eruptions (Foshag and González, 1956; Andronico et al., 2005; Thorarinsson and Sigvaldason, 1972), determining progressive sealing of the non-active portions of the fissure.

Non-homogeneous cooling and crystallization of magma along the fissure can determine flow localization and the evolution toward central eruptions (Bruce and Huppert, 1989; Wylie et al., 1999; Wylie and Lister, 2006). However, flow localization has also been observed in very early eruption stages and in very energetic eruptions, when the effects of magma cooling and solidification are less relevant. It is well known that the geometry of volcanic conduits significantly affects the shearing geometry of magmatic flows and the distribution of horizontal and vertical velocity gradients. In the case of separate two-phase flow (i.e., when gas bubbles rise within low-viscosity magmas), shearing effects determine lateral gas segregation and can have a primary control on the flow pattern and phase distribution, eruption dynamics, and vent location. These effects are neglected in most volcanic conduit flow models, which usually assume vertical axial symmetry of the flow field (Gonnermann and Manga, 2007).

For these reasons, the characterization of properties and stability of flow patterns is fundamental to quantify flow dynamics. Existing computational fluid dynamics models of separate multiphase flows within fissure-like systems (Pan et al., 2000; Joshi et al., 2002) are calibrated against experimental data obtained at very different dynamic regimes (i.e., water-gas flows) and cannot be directly applied to real eruptions. Dedicated experimental activity is essential to fill this gap and provide the necessary physical constraints to model magma flows. The purpose of this paper is to present results from scaled experiments aimed at exploring the stable configurations of separate two-phase flow regimes in mafic magmas along fissures and compare them with flow dynamics in cylindrical conduits.

EXPERIMENTAL APPARATUS

Experiments were performed on a 1.5-m-high × 0.75-m-wide × 0.03-m-thick rectangular bubble column at the University of Geneva (Switzerland). Air (from 2 to 80 L/min) was injected at the bottom of the column through equally spaced nozzles. Experiments were carried out with either water or aqueous solutions of glucose syrup at different concentrations, with viscosities ranging from 10^{-1} to 70 Pa·s. Pressure was measured with a system of six transducers mounted in rows of threes at 0.5 and 1 m from the base of the column. Visual observations and high-speed recording of the flow were aimed at evaluating the bubble distribution in the column and the average and instantaneous column heights attained by the mixture of gas and liquid during the flow. These data were used to discriminate different flow regimes, assess transitions, and calculate the gas fraction in the mixture by comparing the height reached by unaerated liquid and the mixture during the runs. Scaling of the experiments with respect to magmatic flow conditions was checked through several dimensionless parameters. Further details on the apparatus, experimental techniques, and scaling considerations are reported in Item DR1 in the GSA Data Repository[1].

RESULTS

Flow Pattern Map

Experimental results showed that two main patterns occurred within the column: (1) homogenous bubbly flow (for gas flow rates <5 L/min and almost all liquid viscosities), with non-interacting multiple bubble chains developing from each nozzle, and (2) bubble plume patterns, where all bubbles rapidly converged toward the center to form a coherent plume with large-scale, gas-driven liquid circulation cells, developing at both sides into circular to elongated geometries, complementary to plume geometry (Fig. 1). Increasing liquid viscosity increased the size of the bubbles in the stream, which were subjected to repeated coalescence and breakup during rise. In particular, at constant gas flow

*E-mail: laura.pioli@unige.ch
†Deceased

[1]GSA Data Repository items 2017249, Item DR1 (experimental techniques and apparatus), Item DR2 (experimental regimes at Ka = 169), and Item DR3 (experimental pressure gradients for selected experiments), is available online at http://www.geosociety.org/datarepository/2017/ or on request from editing@geosociety.org.

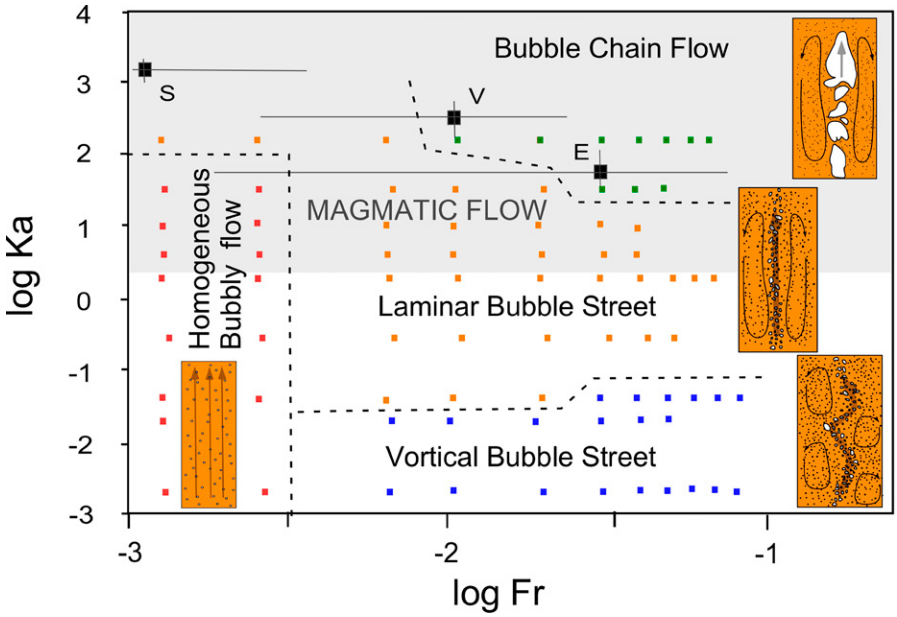

Figure 1. Flow map. Experiments are marked by small squares; colors differentiate flow regimes. Gray area marks expected conditions for flows of mafic magmas. Black squares indicate average outgassing conditions at vent at open conduit for the following volcanoes: S—Stromboli (Italy); V—Villarrica (Chile); E—Etna (Italy). Superficial gas velocity is gas volume flow rate divided by cross section area of tank. Ka—Kapitsa number; Fr—Froude number. Representative drawings of each flow regime are shown (white is gas, orange is liquid).

rates, the largest bubble measured in the flow increased in size with increasing liquid viscosity (Fig. 2). The different trends in size showed by the largest measured bubbles and the bubbles forming at the nozzles suggest that coalescence effects are not uniform and likely affected by the flow patterns (Fig. 2).

In high-viscosity liquid experiments, a marked bimodality of bubble sizes existed between the central stream, with centimeter-scale bubbles, and the peripheries, where microvesicular liquid circulated within convection cells. The smallest bubbles dispersed in the liquid originated at the liquid-free surface from the burst of large bubbles and incomplete retraction of the liquid film, as observed by Bird et al. (2010) and Pioli et al. (2012). Figure 1 shows the stability field of specific flow patterns observed when the gas was uniformly injected and in terms of two key dimensionless parameters: the Kapitsa (Ka) and the Froude (Fr) numbers. Ka quantifies the ratio of surface tension forces to inertial forces (Kapitsa, 1948) and corresponds to:

$$\mathrm{Ka} = \left[\frac{g\eta^4\Delta\rho}{\rho_l^2\sigma^3}\right]^{0.25}, \quad (1)$$

where g is the acceleration of gravity, η is the liquid viscosity, ρ and σ are the liquid density and surface tension, respectively, and $\Delta\rho$ is the difference in density between gas and liquid.

Fr, quantifying the ratio of inertial to gravitational forces, corresponds to

$$\mathrm{Fr} = \frac{u_{sg}}{\sqrt{gD}}, \quad (2)$$

where u_{sg} is the superficial gas velocity, which is the ratio between the gas volume flow rate and the cross section area of the conduit, and D is the hydraulic diameter of the column. "Homogenous flow" patterns were observed at any Ka for Fr < 0.05. For higher Fr, bubble streams started interacting and neighboring bubble streams coalesced with each other, forming bubble plumes that gradually converged toward the center of the column. Two main liquid circulation cells developed at both sides of the column. This pattern has been called "laminar bubble street" (Rietema and Ottengraf, 1970). For the lowest liquid viscosities (i.e., <0.01 Pa·s), the bubble stream was wavy and not stationary (i.e., it was subjected to periodical oscillations by the formation of temporary, smaller liquid circulation cells at the column sides; Fig. 1). This pattern was called "vortical bubble street." Finally, for flows involving liquids with viscosities >15 Pa·s and u_{sg} of 0.003 m/s or larger, bubble coalescence led to the formation of a chain of large bubbles at the middle of the column. These bubbles were the largest observed in the experimental runs. This pattern was called "bubble chain flow." When gas was inserted only from the central nozzles, stable bubble plumes formed even at the lowest gas flow rates.

Time-Averaged Flow Properties

With increasing superficial gas velocities or liquid viscosity, the average properties of the flow vary with trends similar to those of cylindrical bubble columns. The average vesicularity increases with increasing gas volume flow rate and liquid density (Fig. 3A), and, in the investigated experimental range, ranged from 0.1 to 15 vol%, measured with an uncertainty increasing with increasing gas flow rates because of larger oscillations of the free surface of the liquid (Fig. 3A). There is a net increase in vesicularity with

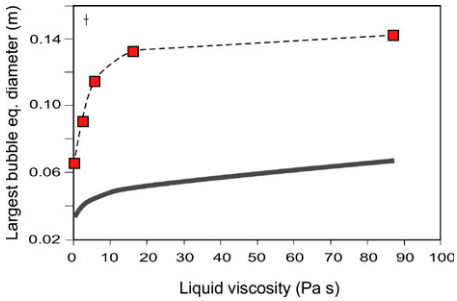

Figure 2. Equivalent (eq.) diameter of largest bubble (red squares; calculated from image analysis) versus liquid viscosity in experiments with Froude number Fr = 0.02–0.03. Gray line represents size of bubbles forming at nozzles, calculated after Gaddis and Vogelpohl (1986). Cross on top left indicates error in measurements.

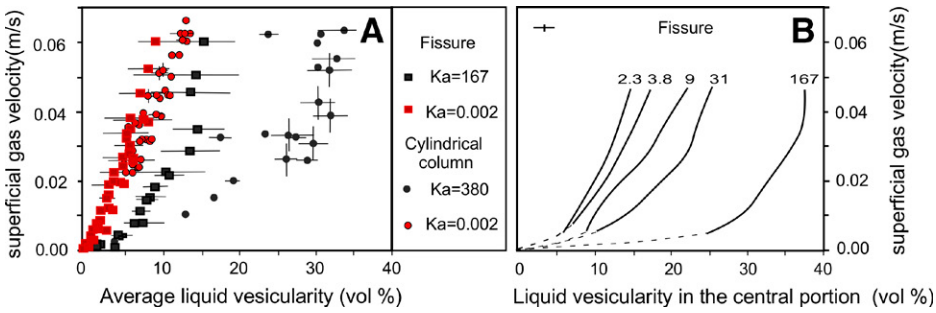

Figure 3. A: Average liquid vesicularity versus superficial gas velocity in outgassing experiments. Errors are shown as bars parallel to axes; if not visible, they are smaller than symbol. Squares refer to experiments done in apparatus described in this paper; circles refer to experiments in cylindrical conduits by Pioli et al. (2012). Ka—Kapitsa number. B: Vesicularity in central plume structure in rectangular column experiments versus superficial gas velocity for various liquid. Numbers indicate Ka values for each set of experiments. Cross on top left indicates error in measurements. Dashed lines are extrapolated patterns.

increasing both Fr and Ka, with low-viscosity liquids showing a monotone increase, and pure glucose syrup reaching a plateau between 14 and 16 vol% at $u_{sg} > 0.03$ m/s. The number and arrangement of gas inlets did not affect these results, and flow pattern shifts determined no apparent discontinuities in the trend.

The pressure drop in the column was primarily controlled by the liquid vesicularity, and because of the non-homogeneous distribution of vesicles in the flow, the pressure gradients inside the fracture varied laterally according to the flow pattern geometries. In general, vertical pressure gradients measured at very low gas flow rates (<5 L/min) were uniform along the column, but they varied laterally for higher Fr and Ka (Item DR2). Lateral variations were highest for single bubble chain flows, where the lowest pressure gradient was attained at the center of the column, reflecting bubble distribution patterns (Fig. 3B). In vortical bubble street patterns, there was a less regular distribution; the lowest pressure drop was attained at either the center or at the periphery of the column, suggesting that the time-averaged pressure drops were balanced by the lateral oscillations of the central plume. In all of the experiments, the lateral variation of pressure drop stabilized to a maximum value at the highest gas flow rates ($u_{sg} > 0.04$ m/s), in analogy to the average vesicularity of the mixture. The vesicularity within the central plume structures (estimated from the pressure drop measured in the central sensors) was up to three times larger than the vesicularity averaged over the entire column, but followed similar trends, with linear increase with superficial gas velocity at low Ka, and strong nonlinear behavior at high Ka (Fig. 3B).

EXPECTED REGIMES IN MAGMATIC FLOWS

Magmatic flows occur at Ka between 10^0 and 10^2 (for magma densities of 2800 kg/m^3, surface tension of 0.08 N/m, and viscosities between 10^0 and 10^3 Pa·s; Gardner et al., 2013), corresponding to the highest-viscosity liquids employed in the experiments. Because of the difficulty in measuring the absolute mass of gas emitted at the vent, only a few data exist on the average outgassing rates at open-vent volcanoes. Average conditions measured at Villarrica (Chile), Etna, and Stromboli (Italy) volcanoes (after Shinohara and Witter, 2005; Aiuppa et al., 2008, 2010) correspond to Fr at the vent between 0.001 and 0.1. Lower Fr is expected at higher depths due to pressure and gas density increase. When plotted on the flow regime chart (Fig. 1), it appears that magmatic flows should occur in the chain flow and laminar bubble street regimes. Both regimes are marked by the occurrence of stable central bubble plume configurations, with slug-like bubbles (i.e., bubbles with a strongly flattened shape, with one dimension comparable with the fissure width) expected for large Ka. However, in analogy with slug flows (i.e., the flow patterns marked by the rise of equally spaced gas slugs in the conduit), this particular regime's stability is also a function of the fracture width and the size of the largest stable bubble (Suckale et al., 2010); in other words, it can occur only if bubbles with thickness comparable with the fracture width are stable in steady flow conditions. Due to the lack of general models, this remains an unsolved point; however, as we will discuss later, it has minor implications when modeling most of the key properties of the flow. In all cases, magma outgassing or gas segregation within fissures will rapidly lead to bubble clustering and the formation of stable vertical bubble plumes, and the onset of lateral gradients in the flow.

Effect of Conduit Geometry on Flow Properties

To understand the effect of conduit geometry on the flow dynamics, it is necessary to compare the experimental results obtained with this two-dimensional column apparatus with similarly scaled outgassing experiments in cylindrical pipes (Fig. 3A; Pioli et al., 2012; Azzopardi et al., 2014). Results suggest that outgassing within fissures is marked by lower vesicularities (up to ~15 vol%), which vary with similar patterns with respect to flows in cylindrical conduits, and the difference increases with increasing Ka. The gas drift flux model predicts that the gas volume fraction ε_g changes as a function of superficial gas velocity and gas drift velocity v_{gd} (i.e., the rise speed of bubbles in the liquid), modulated by a distribution parameter C_0 which is a function of the velocity profile in the conduit (Zuber and Findlay, 1965; Wallis, 1969):

$$\mu_g = \frac{u_{sg}}{C_0 u_{sg} + v_{gd}}. \quad (3)$$

Assuming similar gas drift velocities, differences in vesicle content arise from a steeper velocity profile in the elongated conduit. This assumption is supported by the experimental observations, which also suggest stronger lateral variations for the more "clustered" chain flow and laminar bubble street regimes. Based on experimental data, we calculate C_0 of 6.9 ± 0.7 for high-Ka flow experiments (Item DR1). However, the average vesicularity is only a reference value and is not representative of any real liquid parcel in our experiments or magma in the fissure. Our experiments show that the vesicularity within the plume structure increases with both gas flow and liquid viscosity, reaching values up to 35% for Ka on the order of 10^2 (Fig. 3B). The steeper velocity and vesicularity profiles are also associated with stronger lateral pressure gradients, which are expected to increase with increasing gas flow and melt viscosity. Finally, bubble clustering and central plume formation enhance also the drag on the liquid, with the formation of stable convection cells (Fig. 4). The occurrence of plume-driven convection cells has important effects on magma mixing and homogenization within the fracture. Image analysis suggests that these hydrodynamic structures involved up to 70 vol% of the liquid in the column in the single bubble chain patterns, and up to 50 vol% in the vortical plume patterns. Recirculation is expected to be much less relevant within cylindrical conduits: for similar Ka, experimental results of Azzopardi et al. (2014) have shown that the fraction of liquid flowing down due to bubble movement increases with decreasing melt viscosity, decreasing superficial gas velocities (which control the rise speed of gas), and increasing conduit diameter, and for similar Fr, it corresponds to ~30 vol%, suggesting a much less efficient induced recirculation. It is worth noting that it is expected that multiple, regularly spaced plumes will develop in fractures whose length exceeds the maximum attainable lateral extent of a single plume unit: spacing between plumes is mainly controlled by the fracture depth. According to Beek (1965), this spacing is approximately twice the dike depth, which would suggest that only longer and/or shallower fissures could develop multiple eruptive centers contemporaneously.

FINAL REMARKS

Gas segregation and multiphase flow processes play a fundamental role in magmatic flow and in the eruptive dynamics of mafic magmas. Gas segregation is enhanced by low magma viscosity, which controls bubble rise speed, and low surface tension, which controls bubble coalescence. We note that our experimental results do not take into account topographic effects on the geometry of the fissure opening (i.e., uneven topography determining partial opening of the dike to the surface), which would have strong

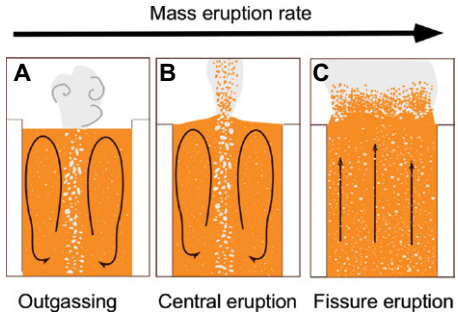

Figure 4. Expected regimes in fissure eruptions. A: Pure outgassing accompanied by magma convection; Froude number, Fr > $10^{-2.5}$. B: Central eruptions either in Strombolian or Hawaiian regimes; gas segregation is still effective in formation of central bubble plume; Fr > $10^{-2.5}$. C: Fissure eruptions (fire curtains); large mass eruption rate (MER) or very low gas flow rate (Fr < $10^{-2.5}$) prevent efficient lateral magma segregation.

influence on local pressure gradients and significantly affect the upper plume dynamics and position within the fissure. Moreover, this model does not take into account the effect of magma fragmentation on the flow distribution, and can be applied directly only to mildly to low-explosive regimes marked by very shallow magma fragmentation, i.e., lava fountains and Strombolian jets. The experiments, however, give important insights into the dynamics of gas segregation in low-viscosity magmas.

Separate two-phase flow controls magma vesicularity in the conduit, which can be directly related to outgassing rates and magma properties. Permeability of viscous magmas, as in porous rocks, is a function of bubble concentration and texture (Rust and Cashman, 2004; Burgisser and Gardner, 2004) and affects outgassing and fragmentation, whereas in low-viscosity magmas, gas does not escape through interconnected bubbles but as discrete bubbles moving through the melt. At any time the bubble content and size distribution is a function of the gas outflow rate and the flow pattern (Zuber and Findlay, 1965; Wallis, 1969). The flow pattern is, in turn, controlled by the conduit geometry and the magma physical properties and viscosity. In other words, the outgassing rate controls the vesicularity of the magma. Gas bubble content increases with increasing melt viscosity (as its ability to "slow down" bubbles increases) and with the gas output. Conduit geometry has primary effects on the development of flow pattern, which, in turn, controls the distribution of gas and melt within the conduit and the bubble rise dynamics. Conduit geometry in the form of a fissure is associated with more efficient gas segregation with respect to cylindrical conduits due to bubble clustering and bubble plume formation, accompanied by bubble-poor melt convection at both sides of the plume (Fig. 4). Even in pure outgassing regimes (Fig. 4A), very low gas flow rates ($Fr > 10^{-1}$) are sufficient to induce stability of bubble plume patterns and efficient, gas-driven magma convection, favoring system homogeneity and stability. If the net liquid flow rate is above zero, in parallel, central eruptions and Strombolian eruptive regimes are expected (Fig. 4B), and gas segregation is still effective in the formation of a central bubble plume. The eruptive activity is then expected to focus in the center of the fissure. Multiple plume formation is expected in fissures characterized by length/depth ratios <4 (Beek, 1965). Conditions for continuous eruptions from fissures (i.e., fire curtains) are possible only when gas segregation is suppressed by large MERs, which prevent the onset of separate rise of gas bubbles within the melt (high MER, possibly $>10^5$ kg/s; Pioli et al., 2009), and/or at very low gas flow rates (i.e., degassed magma, $Fr < 10^{-2.5}$).

When compared with cylindrical conduit patterns developing at similar conditions (i.e., Ka and Fr values), flows in fissures are expected to induce more efficient liquid convection at the peripheries involving magma volume fractions more than twice as large, favoring homogeneity of the magma and stable dynamic conditions. Increase in viscosity of the melt increases plume size because larger gas bubbles, vesicularity, and lateral pressure gradients are expected, favoring lateral gas segregation.

ACKNOWLEDGMENTS

The research was supported by Fond National Suisse grant 200020-132543. We are grateful to Mr. F. Arlaud for the final design and construction of the experimental rig. The editor, K. Genareau, and two anonymous reviewers are acknowledged for constructive comments and criticism. We dedicate this paper to the memory of B. Azzopardi, whose enthusiasm and dedication were essential to this research. We will miss him greatly.

REFERENCES CITED

Aiuppa, A., Giudice, G., Gurrieri, S., Liuzzo, M., Burton, M., Caltabiano, T., McGonigle, A.J.S., Salerno, G., Shinohara, H., and Valenza, M., 2008, Total volatile flux from Mount Etna: Geophysical Research Letters, v. 35, L24302, doi:10.1029/2008GL035871.

Aiuppa, A., Bertagnini, A., Métrich, N., and Moretti, R., 2010, A model of degassing for Stromboli volcano: Earth and Planetary Science Letters, v. 295, p. 195–204, doi:10.1016/j.epsl.2010.03.040.

Andronico, D., et al., 2005, A multi-disciplinary study of the 2002–03 Etna eruption: Insights into a complex plumbing system: Bulletin of Volcanology, v. 67, p. 314–330, doi:10.1007/s00445-004-0372-8.

Azzopardi, B.J., Pioli, L., and Abdulkareem, L.A., 2014, The properties of large bubbles in very viscous liquids in vertical columns: International Journal of Multiphase Flow, v. 67, p. 160–173, doi:10.1016/j.ijmultiphaseflow.2014.08.013.

Beek, W.J., 1965, Oscillations and vortices in a batch of liquid sustained by a gas flow, *in* Proceedings, Symposium of Two Phase Flow, Exeter, UK, 21–23 June.

Bird, J.C., Ruiter, R., de Courbin, L., and Stone, H.A., 2010, Daughter bubble cascades produced by folding of ruptured thin films: Nature, v. 465, p. 759–762, doi:10.1038/nature09069.

Bruce, P.M., and Huppert, H.E., 1989, Thermal control of basaltic fissure eruptions: Nature, v. 342, p. 665–667, doi:10.1038/342665a0.

Burgisser, A., and Gardner, J.E., 2004, Experimental constraints on degassing and permeability in volcanic conduit flow: Bulletin of Volcanology, v. 67, p. 42–56, doi:10.1007/s00445-004-0359-5.

Foshag, W.F., and González, J.R., 1956, Birth and development of Parícutin volcano, Mexico, *in* Segerstrom, K., et al., Geologic Investigations in the Parícutin Area, Mexico: U.S. Geological Survey Bulletin 965, p. 355–489.

Gaddis, E.S., and Vogelpohl, A., 1986, Bubble formation in quiescent liquids under constant flow conditions: Chemical Engineering Science, v. 41, p. 97–105, doi:10.1016/0009-2509(86)85202-2.

Gardner, J.E., Ketcham, R.A., and Moore, G., 2013, Surface tension of hydrous silicate melts: Constraints on the impact of melt composition: Journal of Volcanology and Geothermal Research, v. 267, p. 68–74, doi:10.1016/j.jvolgeores.2013.09.007.

Genareau, K., Valentine, G.A., Moore, G., and Hervig, R.L., 2010, Mechanisms for transition in eruptive style at a monogenetic scoria cone revealed by microtextural analyses (Lathrop Wells volcano, Nevada, U.S.A.): Bulletin of Volcanology, v. 72, p. 593–607, doi:10.1007/s00445-010-0345-z.

Gonnermann, H., and Manga, M., 2007, The fluid mechanics inside a volcano: Annual Review of Fluid Mechanics, v. 39, p. 321–356, doi:10.1146/annurev.fluid.39.050905.110207.

Joshi, J.B., Vitankar, V.S., Kulkarni, A.A., Dhotre, M.T., and Kalekudithi, E., 2002, Coherent flow structures in bubble column reactors: Chemical Engineering Science, v. 57, p. 3157–3183, doi:10.1016/S0009-2509(02)00192-6.

Kapitsa, P.L., 1948, Wave flow of thin layers of a viscous fluid: I. Free flow: Zhurnal Eksperimentalnoi i Teoreticheskoi Fiziki, v. 18, p. 1–28.

Pan, Y., Dudukovic, M.P., and Chang, M., 2000, Numerical investigation of gas-driven flow in 2-D bubble columns: American Institute of Chemical Engineers, v. 46, p. 434–449, doi:10.1002/aic.690460303.

Pioli, L., Azzopardi, B.J., and Cashman, K.V., 2009, Controls on the explosivity of scoria cone eruptions: Magma segregation at conduit junctions: Journal of Volcanology and Geothermal Research, v. 186, p. 407–415, doi:10.1016/j.jvolgeores.2009.07.014.

Pioli, L., Bonadonna, C., Azzopardi, B.J., Phillips, J.C., and Ripepe, M., 2012, Experimental constraints on the outgassing dynamics of basaltic magmas: Journal of Geophysical Research, v. 117, B03204, doi:10.1029/2011JB008392.

Reynolds, P., Brown, R.J., Thordarson, T., and Llewellin, E.W., 2016, The architecture and shallow conduits of Laki-type pyroclastic cones: Insights into a basaltic fissure eruption: Bulletin of Volcanology, v. 78, 36, doi:10.1007/s00445-016-1029-0.

Rietema, K., and Ottengraf, S., 1970, Laminar liquid circulation and bubble street formation in a gas-liquid system: Transactions of the Institution of Chemical Engineers, v. 48, p. 54–62.

Rust, A., and Cashman, K.V., 2004, Permeability of vesicular silicic magma: Inertial and hysteresis effects: Earth and Planetary Science Letters, v. 228, p. 93–107, doi:10.1016/j.epsl.2004.09.025.

Shinohara, H., and Witter, J., 2005, Volcanic gases emitted during mild Strombolian activity of Villarrica volcano, Chile: Geophysical Research Letters, v. 32, L20308, doi:10.1029/2005GL024131.

Suckale, J., Hager, B.H., Elkins-Tanton, L.T., and Nave, J.-C., 2010, It takes three to tango: Bubble dynamics in basaltic volcanoes and ramifications for modeling normal Strombolian activity: Journal of Geophysical Research, v. 115, B07410, doi:10.1029/2009JB006917.

Thorarinsson, S., and Sigvaldason, G.E., 1972, The Hekla eruption of 1970: Bulletin of Volcanology, v. 36, p. 269–288, doi:10.1007/BF02596870.

Wallis, G.B., 1969, One-Dimensional Two-Phase Flow: New York, McGraw-Hill, 410 p.

Wylie, J., and Lister, J., 2006, The effects of temperature-dependent viscosity on flow in a cooled channel with application to basaltic fissure eruptions: Journal of Fluid Mechanics, v. 305, p. 239–261, doi:10.1017/S0022112095004617.

Wylie, J., Helfrich, K., Dade, B., Lister, J.R., and Salzig, J.F., 1999, Flow localization in fissure eruptions: Bulletin of Volcanology, v. 60, p. 432–440, doi:10.1007/s004450050243.

Zuber, N., and Findlay, J., 1965, Average volumetric concentration in two-phase flow systems: Journal of Heat Transfer, v. 87, p. 453–468, doi:10.1115/1.3689137.

Manuscript received 10 November 2016
Revised manuscript received 20 April 2017
Manuscript accepted 25 April 2017

Printed in USA